

Planar optical waveguides for interconnection of VLSI

J.S. Wilkinson, S. Hao, D. Murphy & J.G. Smith

Department of Electronics & Computer Science,
The University, Southampton, SO9 5NH,
United Kingdom

N. Nourshargh & N. Howard

GEC Research Ltd.,
East Lane, Wembley, Middlesex, HA9 7PP,
United Kingdom

Abstract

Optical interconnection offers improved performance of VLSI circuits and systems. Planar optical waveguides allow interconnections to be printed directly onto optical circuit boards. The experimental assessment of waveguide options is discussed. Combinations of waveguide bends and intersections have been modelled, and experimental results are given.

Introduction

Conventional metallic interconnections limit the performance of VLSI circuits and systems. In particular, capacitive loading of striplines by multiple fanouts limits operating speed; and low bandwidth, combined with crosstalk-constrained interconnect density, limits the I/O capacity of chips. Optical interconnection offers the potential for improved fan-out, greater bandwidth, immunity from crosstalk, increased interconnection density, reduction of planar layout constraints, freedom from electromigration and reduction in pin-count^{1,2}.

Optical interconnection techniques may be categorised as either (a) Guided; with optical fibre or planar waveguide distribution, or (b) Unguided; with broadcast or focused distribution. In this paper we consider only planar optical waveguides for chip-to-chip connection. Planar waveguides are attractive because a complete interconnection network may be printed photolithographically, allowing relatively simple fabrication technology together with simultaneous registration between all the optical ports on a chip and the waveguides on the printed optical circuit. A key advantage of planar optical waveguides is that they may pass through each other with low loss and low crosstalk, relaxing layout constraints. Multilayer construction is also possible.

Printed optical circuits for optical interconnection of VLSI require simple inexpensive techniques for fabricating planar waveguides. Waveguide components such as bends, junctions, intersections and couplers must be optimised for interconnection topologies. A number of waveguide materials for the printed optical circuit have been investigated, these include:

- (a) Laser-machined doped silica waveguides.
- (b) Screen-printed glass waveguides.
- (c) Ion-exchanged waveguides in glass.

The two former waveguide options have been characterised using simple multimode waveguides and Y-junctions, while bends and crossovers have been investigated using ion-exchanged waveguides.

The performance of the inter-chip link is largely determined by the power budget. In order to predict performance and find design rules for the printed optical circuit, the optical losses of combinations of multimode waveguide bends and intersections have been modelled. Experimental results for an example configuration have been obtained using silver ion-exchanged waveguides, whose basic properties have been well known for many years.

Laser-machined doped silica waveguides

A novel laser machining technique for fabricating integrated optical circuits in doped silica has been developed. The "direct-write" nature of this technique eliminates the need for photolithography, etching, etc. thereby making fabrication simple. Another very important and unique feature of these waveguides is that they are composed of much the same material as optical fibres, and should therefore have very similar characteristics, such as very low attenuation and very high stability.

The waveguide fabrication technique consists of two stages: deposition of a doped silica film on a silica substrate, followed by CO₂ laser machining of the film to produce the

desired pattern of strip waveguides. A microwave plasma-assisted CVD technique^{3,4} is used to deposit on a silica substrate, a glassy layer of silica doped with germania and fluorine. For the present application, the deposited films typically have a thickness of around 20 μm and a Δn of approximately 0.01 with respect to the silica substrate whose typical dimensions are 10 x 30 x 1 mm³. The planar waveguide thus formed is then processed to produce the desired pattern of strip waveguides. For this purpose, we use the apparatus shown schematically in Figure 1. The output of a CO₂ laser is focused onto the planar waveguide which is mounted on a computer-controlled X-Y translation stage. By adjusting the laser power and the scanning speed of the translation stage, one can ensure that sufficient heat is absorbed to cause localised vapourisation of the film and hence the formation of a groove⁵. Typically a scanning speed of 1 cm/s is used together with 20W of laser power focused through a lens with a focal length of 25mm. Two parallel grooves are cut into the film, the region between them forming a strip waveguide, as shown in Figure 2. Complex patterns of waveguides can be readily produced by programming the computer to generate the required movements of the X and Y axes of the translation stage. A typical printed optical circuit consisting of several waveguide beam-splitters, for example, can be "written" in a few seconds.

Both straight waveguides and Y-junction beam-splitters have been fabricated using this technique. The straight waveguides have an attenuation of approximately 1dB/cm at $\lambda = 0.6328\mu\text{m}$, while the Y-junctions shown in Figure 3 introduce an extra loss of typically 5dB. The attenuation of the planar waveguides into which these structures were cut were typically less than 0.2dB/cm. The increased loss of the straight waveguides is largely due to redeposition of some of the vapourised glass as silica powder on the top surface of the waveguide, which then suffers a larger scattering loss. On the other hand, the excess loss of the Y-junction is largely determined by the "sharpness" of the branching point. The finite minimum spot size (@50 μm) of the focused beam from the CO₂ laser has the effect of blunting the branching point and thus causing extra loss. A theoretical study is currently in progress to establish the expected magnitude of this excess loss.

These are preliminary results which can be substantially improved by optimising the laser-machining process. For example, by depositing a cladding layer on the waveguide prior to laser-cutting, the effects of the two loss mechanisms described earlier may be dramatically reduced.

Screen-printed glass waveguides

Commercially available screen-printed glass was developed as a sealant for electronic packages and for producing layers of dielectric for multilayer hybrid integrated circuit substrates. Thick film optical waveguides using such glasses have been demonstrated⁶, and part of our work has been directed towards fabricating waveguides with sufficiently low loss for optical interconnection.

The advantages of using screen-printed glass waveguides are that they take advantage of an established method of producing printed electrical circuits, that the waveguides are produced directly and inexpensively on an established hybrid thick-film substrate, and that the glass is thermally matched to an alumina substrate. Electrical components are easily added to this substrate to form a printed optical circuit assembly. Screen-printed glass waveguides have also been demonstrated on borosilicate glass substrates. This alternative process has the advantage of allowing the elimination of one layer of screen-printed glass.

Waveguide fabrication

The structure of the waveguides is shown in Figure 4. The waveguides were produced by screen-printing a low-index buffer layer of Hereaus IP 041 paste ($n = 1.69$) onto an alumina substrate. The material was then prebaked in vacuum at 150°C for 10-15 minutes, before being fired in a 4 zone belt furnace at a peak firing temperature of 580-620°C to produce a clear and smooth glass. To complete the structure, 100 μm wide tracks of EMCA glass 92 paste ($n = 1.82$ when fired) were screen-printed onto the low index glass layer. This material was also prebaked in a vacuum before being fired at a peak firing temperature of 580-620°C to form the complete waveguide structure. Both layers of glass were screen-printed using a stainless steel mesh of 157 lines/cm.

Figure 5 shows a SEM photograph of a fractured edge of a screen-printed glass waveguide, and Figure 6 shows the surface profile of such a waveguide. The Figures show that the guiding regions have an approximately parabolic profile, as a result of the flowing of the glass during firing. The thickness of the guiding regions is typically 6-8 μm , and the width typically 150-300 μm . Thicker waveguides can readily be produced, and the waveguide width may be reduced to 100 μm , or 50 μm if a non-mesh mask is used. Measurements show that the surface roughness of the printed waveguides is approximately 20nm.

Measurements

Light with a wavelength of $0.6328\mu\text{m}$ was launched into the waveguide from an optical fibre, and by focusing onto the fractured, unpolished, edge of the waveguide. The optical loss of the waveguide was determined by measuring the light scattered from the waveguide as a function of distance along the guide. The loss of straight sections of these waveguides is less than 5dB/cm .

This loss compares favourably with previously published results⁶. These waveguides have been fabricated using established screen-printing techniques and materials, not developed for optical devices. We therefore expect that the losses may be reduced by improving the edge definition of the screen-printing process, and by developing the materials to improve their optical properties, by reducing their impurity content.

Ion-exchanged waveguides in glass

Ion-exchange in glass is a simple and inexpensive method of fabricating stable, durable, planar waveguides⁷. Silver ion-exchanged waveguides exhibit rather high loss ($>2\text{dB/cm}$), but have the potential for high numerical aperture (up to 0.5), and the advantages of low process temperature ($250^\circ\text{C} - 300^\circ\text{C}$) and low toxicity. Thallium ion-exchanged waveguides have a similar N.A. and process temperature, and very low loss ($<0.1\text{dB/cm}$); however the toxicity of the process is high. Channel waveguides may be defined photolithographically, and optoelectronic devices on VLSI chips may be aligned with waveguides on the printed optical circuit using depressions machined or etched into the glass.

Waveguide bends and intersections

Waveguide bends and intersections inevitably exhibit some loss, but to become feasible, optical interconnections must show low loss and low crosstalk. Ion-exchanged waveguides have been chosen as a vehicle to study the trade-offs which exist in the design of combinations of waveguide bends and intersections, as they have been well characterised.

A simple ray-optical approach, suitable for multimode waveguides, has been adopted to study these components. Waveguide bends have been modelled using the analysis of Winkler et al.⁸, and intersections have been modelled using the approach of Kurokawa et al.⁹. A computer program has been written which combines these two analyses, and determines the loss suffered by light propagating in the structure shown in Figure 7. In this approach it is assumed that the waveguides have a step index profile, and that the waveguide input aperture is filled uniformly. The scattering and absorption losses in the waveguides are not considered in this model.

A trade-off exists between bend loss and intersection loss (assuming that the substrate index, n_s , remains constant) because

- (a) Bend loss - decreases with increasing core index, n_c
 - decreases with increasing R/w
 - increases with increasing angle, ψ
- (b) Intersection loss - increases with increasing core index, n_c
 - decreases with increasing angle, ψ

Theoretical results are shown in Figures 8 and 9, for waveguides with substrate index, n_s , of 1.51 and core index, n_c , of 1.6, corresponding to simple silver or thallium ion-exchanged waveguides in soda-lime glass. It is assumed that the waveguides have a step index profile, which may be obtained if field-assisted ion-exchange is used. The wavelength being considered is $0.85\mu\text{m}$, being within the range of emission of GaAlAs devices, which are suitable for optical interconnection of silicon VLSI. Results for a wavelength of $0.6328\mu\text{m}$ are lower than these, but within 0.1dB over the range considered. Figure 8 shows the loss in this structure for a range of waveguide widths as a function of bend angle, ψ , for a bend radius of 0.5mm . Figure 9 shows similar curves for a bend radius of 2.00mm . Bend/intersection angles smaller than 20° have not been considered, as crosstalk would then be inevitable between waveguides with these indices.

For sufficiently small ratios of waveguide width to radius of curvature (w/R), the intersection loss is dominant, and losses are minimised by using 90° intersections. As w/R is increased, however, a smaller angle becomes optimum. Figure 8 shows a slight increase in loss with angle, beyond approximately 80° , for the two widest waveguides. However, the total loss in these cases is too high to be of practical interest for optical interconnection and it is apparent that for low loss, using media with these refractive indices, 90° bend/intersections are most attractive. Small waveguide width and large radius of curvature are advantageous, but consideration must be given to input coupling efficiency, tolerance to misalignment between printed optical circuit and chip, and constraints on circuit layout,

before these may be determined.

Figure 10 shows the loss of the combined structure against waveguide core index, for a fixed substrate index. The waveguide width is $50\mu\text{m}$, the bend radius is 2.0mm , and bend angles of 20° , 45° , and 90° are shown. For small bend angles a core index somewhat smaller than 1.6 yields the lowest loss, while the lowest loss in the complete range under consideration is obtained using 90° bends and an n_c of 1.6, which is approximately the highest obtainable with silver ion-exchange in standard soda-lime glass substrates.

Figure 11 shows similar curves to those in Figure 10, with the exception that the waveguide width is $20\mu\text{m}$. The losses are lower, due to the reduction in bend loss and, as before, the lowest loss occurs with a 90° bend angle; however, this minimum loss now occurs with a lower core index of approximately 1.59.

The conclusions to be drawn from this simple ray analysis of bending and intersecting waveguides with high N.A. are as follows. If the numerical aperture of the waveguides is filled uniformly, losses are minimised by using 90° intersections, for reasonable values of w/R . Waveguide width is constrained by alignment tolerances, but if narrow guides are used, waveguide losses are lower. For any ratio of waveguide width to bend radius there exists a waveguide core index, for a given substrate, at which losses are minimised in the combined structure. If this ratio is small, for example $w < 25\mu\text{m}$ with $R = 2.0\text{mm}$, this optimum core index falls below the maximum obtainable using silver (or thallium) ion-exchange. In these circumstances it may be worthwhile to employ dilute ion-exchange melts to obtain a lower core index. However, this model does not consider the coupling loss between an emitter and a waveguide, which is a function of core index and which must be included before complete design rules may be established.

Waveguide fabrication

Soda-lime glass substrates having a refractive index of 1.51 and measuring nominally $50 \times 50 \times 1\text{mm}^3$ were used in these experiments. The substrates were cleaned, and 300nm of aluminium was deposited by thermal evaporation. Windows in the form of tracks 10 to $100\mu\text{m}$ wide were opened in this film, using conventional photolithography, to form a diffusion mask. The substrates were then immersed in a silver nitrate melt at 290°C for five hours. The Al film was subsequently removed, and mode measurements showed that the waveguides formed had an index of 1.595 ± 0.005 at the substrate surface, and a depth of approximately $25\mu\text{m}$. The edges of the substrates were polished to allow end-fire coupling of light into the waveguides.

Waveguide patterns 10 , 50 and $100\mu\text{m}$ wide, comprising 90° arcs with radius of curvature ranging from 0.5 to 4.0mm , and combined structures as shown in Figure 6, with guide width of $50\mu\text{m}$, bend radius of 2.0mm and bend/intersection angles of 45° and 90° were fabricated.

Measurements

Measurements were made of straight waveguide loss, bend loss, intersection loss and intersection crosstalk. Light with a wavelength of $0.6328\mu\text{m}$ was end-fire coupled into the waveguides through a polished edge, using a microscope objective lens. Loss measurements were made using a scanning fibre probe¹⁰; the back surface of the substrate was ground and blackened to reduce errors due to stray light in the substrate¹¹. Crosstalk at the intersection was measured by comparison of the power emerging from the polished ends of the waveguides, with the input of only one waveguide excited.

Results

The loss of light propagating in sections of straight waveguide was $2.5\text{dB} \pm 0.4\text{dB}$ for all waveguides measured.

The results for bend losses are given in Table 1. These results were obtained by comparing the scattered light intensities in straight sections of waveguide immediately before and after the waveguide bends, and subtracting the propagation loss of a straight section of that waveguide of equal length. The losses depend upon the launching conditions, resulting in the fairly wide tolerances given for the data. The results for radius of curvature of 1.0mm and 2.0mm are close to those predicted theoretically, while the results for a radius of curvature of 0.5mm are higher than expected. This discrepancy may be due to the graded-index nature of waveguides fabricated. Waveguides fabricated using field-assisted ion-exchange have an index profile closer to a step, and should yield results more closely in agreement with theory.

	w = 50 μ m	w = 100 μ m
R = 0.5mm	10 +/- 5dB	16 +/- 5dB
R = 1.0mm	1.9 +/- 0.5dB	3.8 +/- 1dB
R = 2.0mm	0.5 +/- 0.3dB	1.5 +/- 0.5dB

Table 1 : Losses for 90° waveguide bends

The loss at each intersection was less than the detectable limit of 0.3dB. Similarly, we were unable to detect any crosstalk between the intersecting waveguides, due to the limit set by imperfect input coupling and radiation loss from the waveguides. Consideration of the data shows that the maximum crosstalk under these circumstances is -30dB with respect to the power emitted from the polished end of the excited waveguide.

Conclusions

In this paper we have described the performance of three materials options for planar optical waveguides for interconnection of VLSI. Laser-cut silica waveguides and screen-printed glass waveguides are at an early stage of development, and while losses are somewhat high at present, work is continuing to reduce these. Silver ion-exchanged waveguides are known to have high loss compared with thallium ion-exchanged guides. However, due to the low toxicity of the process and similarity of the waveguides in other respects, we have chosen to use them to study waveguide bends and intersections, which are important components for optical interconnection. Theoretical investigation of a simple example waveguide configuration including bends and intersections leads to the conclusion that for most waveguides with high N.A., 90° bend/intersection combinations exhibit least loss. Further work on emitter-waveguide coupling is required before design rules can be established.

Acknowledgements

This work is part of an ESPRIT project which includes research into many aspects of optical interconnection, including detectors and emitters. The authors would like to thank their collaborators, Telettra SpA, for their contribution to the programme, and the European Community for part funding of this work.

References

1. Goodman, J.W., Leonberger, F.J., Kung, S-Y., and Athale, R.A., "Optical interconnections for VLSI systems", *Proc. IEEE*, Vol. 72, pp. 850-866, 1984.
2. Haugen, P.R., Rychnowsky, S., and Husain, A., "Optical interconnects for high speed computing", *Opt. Eng.*, Vol. 25, pp. 1076-1085, 1986.
3. Nourshargh, N., Starr, E.M., and McCormack, J.S., "Plasma deposition of GeO₂/SiO₂ and Si₃N₄ waveguides for integrated optics", *IEE Proc.*, Vol. 133, Part J, No. 4, pp. 264-266, 1986.
4. Nourshargh, N., and Starr, E.M., "Microwave plasma deposition and etching of integrated optical waveguides", *Proc. 6th Int. Conf. on Ion and Plasma Assisted Techniques*, May 1987, Brighton, UK., pp. 459-463.
5. Nourshargh, N., Arnold, L.J., Starr, E.M., and Fatatry, A.El., "Fabrication of V-grooves in silica using a CO₂ laser", *Proc. IEE Colloq. on Laser Processing of Materials*, pp. 10/1-10/3, Dec. 1986.
6. South, R.B., and McDonough, M., "Thick-film optical waveguides", *Proc. 5th European Hybrid Microelectronics Conf.*, Stresa, Italy, pp. 433-439, 1985.
7. Findakly, T., "Glass waveguides by ion-exchange : a review", *Opt. Eng.*, Vol. 24, pp. 244-250, 1985.
8. Winkler, C., Love, J.D., and Ghatak, A.K., "Loss calculation and design of arbitrarily curved integrated optic waveguides", *Opt. Quant. Electron.*, Vol. 11, p. 173, 1979.
9. Kurokawa, T., and Oikawa, S., "Optical waveguide intersections without light leak", *Appl. Opt.*, Vol. 16, p. 1033, 1977.
10. Nourshargh, N., "Simple technique for measuring attenuation of integrated optical waveguides", *Electron. Lett.*, Vol. 21, p. 818, 1985.
11. De Bernadi, C., Loffredo, A., and Morasca, S., "Optimum conditions for waveguide loss measurements by scattered radiation detection at visible and near-IR wavelengths", *Proc. SPIE Int. Soc. Opt. Eng.*, Vol. 651, pp. 256-262, 1986.

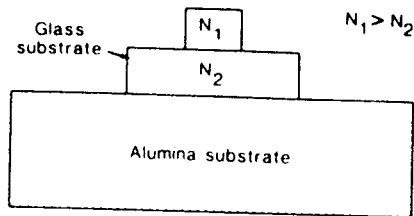


Figure 4 : Schematic structure of screen-printed waveguides

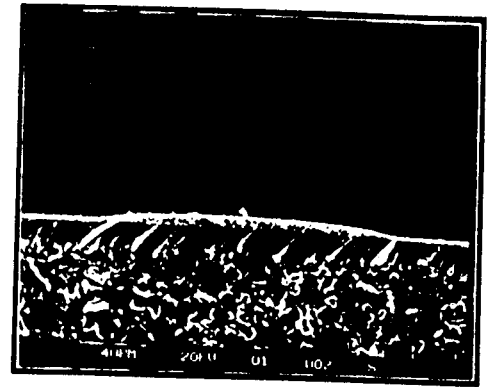


Figure 5 : SEM photograph of screen-printed waveguide cross-section

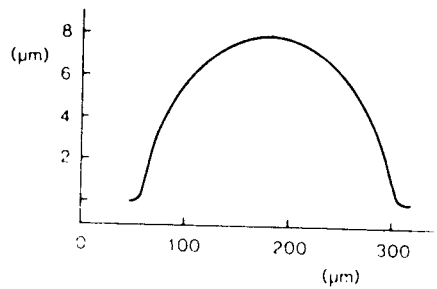


Figure 6 : Surface profile of screen-printed waveguide

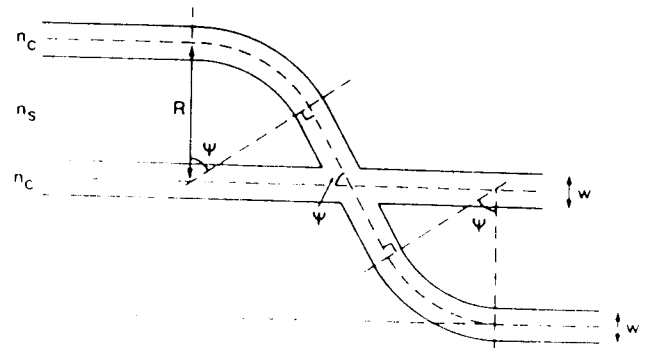


Figure 7 : Combined waveguide structure

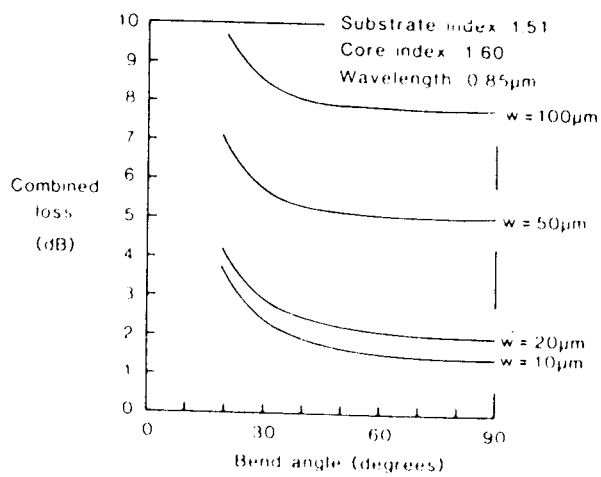


Figure 8 : Loss of combined structure against bend angle Bend radius : 0.5mm

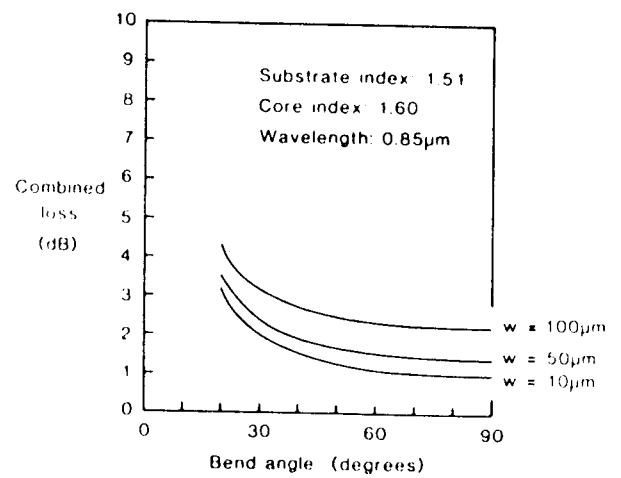


Figure 9 : Loss of combined structure against bend angle Bend radius : 2.0mm

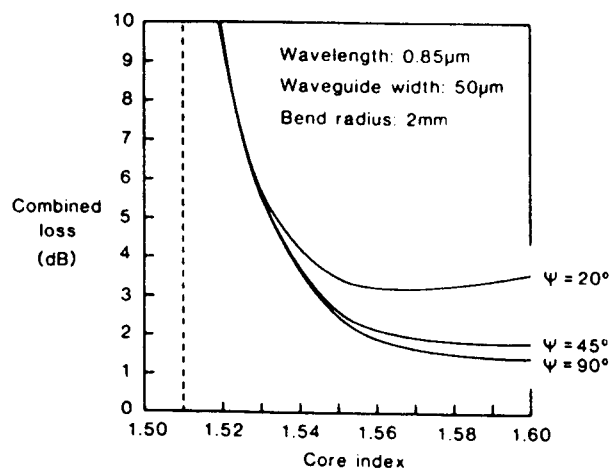


Figure 10 : Loss of combined structure against bend angle. Waveguide width : 50μm.

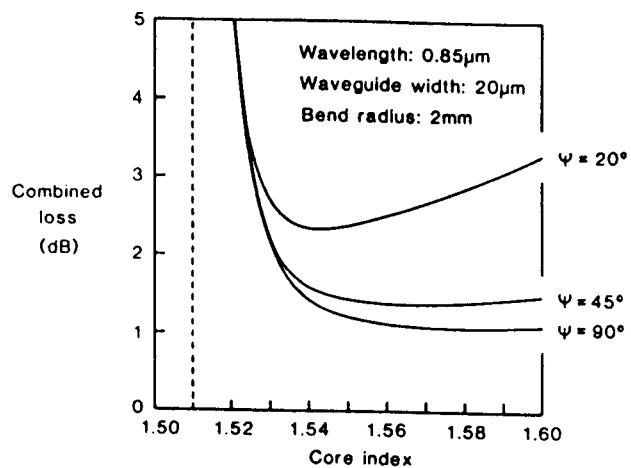


Figure 11 : Loss of combined structure against core index. Waveguide width : 20μm.

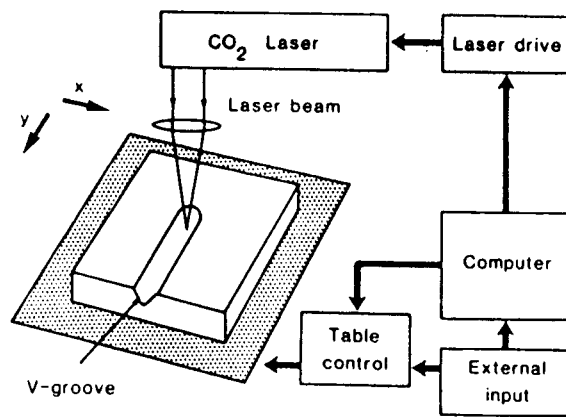


Figure 1 : V-groove fabrication system

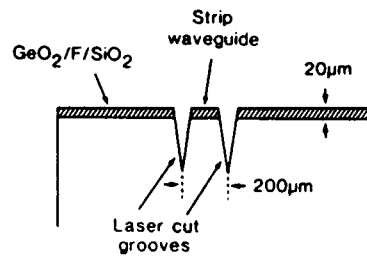


Figure 2 : Schematic structure and near-field output pattern of a straight waveguide

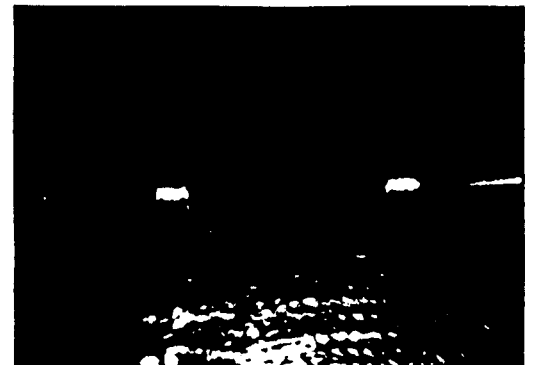
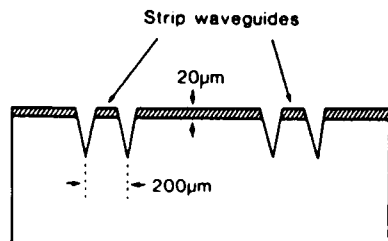


Figure 3 : Schematic structure and near-field output pattern of a waveguide Y-junction